Volume 1 | Number 1 | Jan 2013 | Pages 1–100

Nanoscale

www.rsc.org/nanoscale

ROYAL SOCIETY OF CHEMISTRY

This is an *Accepted Manuscript*, which has been through the Royal Society of Chemistry peer review process and has been accepted for publication.

Accepted Manuscripts are published online shortly after acceptance, before technical editing, formatting and proof reading. Using this free service, authors can make their results available to the community, in citable form, before we publish the edited article. We will replace this *Accepted Manuscript* with the edited and formatted *Advance Article* as soon as it is available.

You can find more information about *Accepted Manuscripts* in the **Information for Authors**.

Please note that technical editing may introduce minor changes to the text and/or graphics, which may alter content. The journal's standard **Terms & Conditions** and the **Ethical guidelines** still apply. In no event shall the Royal Society of Chemistry be held responsible for any errors or omissions in this *Accepted Manuscript* or any consequences arising from the use of any information it contains.

Nanoscale

COMMUNICATION

Chemical Sporulation and Germination: Cytoprotective Nanocoating of Individual Mammalian Cells with Degradable Tannic Acid-Fe[III] Complex

Juno Lee[a], Hyeoncheol Cho[a], Jinsu Choi[b], Doyeon Kim[a], Daewha Hong[a], Ji Hun Park[a], Sung Ho Yang*[b], and Insung S. Choi*[a]

Individual mammalian cells were coated with cytoprotective and degradable films by the cytocompatible processes maintaining the cell viability. Three types of mammalian cells (HeLa, NIH 3T3, and Jurkat cells) were coated with a metal-organic complex of tannic acid (TA) and ferric ion, and the TA-Fe[III] nanocoat effectively protected the coated mammalian cells against UV-C irradiation and a toxic compound. More importantly, the cell proliferation was controlled by programmed formation and degradation of the TA-Fe[III] nanocoat, mimicking the sporulation and germination processes found in Nature.

Nature has developed biological defense mechanisms to protect and maintain the genetic information from natural enemies, diseases, nutrient deprivation, or climate/environmental changes.[1] For example, certain bacteria make themselves highly resistant to unfavorable environments, by forming a robust coat over cell walls as well as shutting down their metabolic activities, in a biological process called 'sporulation'.[2] With this protective coat, the bacterial endospore can survive extreme conditions including UV radiation, desiccation, heat, freezing, and toxic chemicals.[2c,d] Even in a dormant spore state, the cell interacts with the environment and begins to proliferate, when the environment becomes favorable, in a process called 'germination'. Over the past decade, researchers have tried to chemically mimic the sporulation process for non-spore-forming microbial cells by encapsulating them individually within nanometric shells of mechanically tough and chemically stable materials, such as silica,[3] titania,[4] nanotubes,[5] polydopamine,[6] and cross-linked polymers.[7] These cell-in-shell structures—artificial spores—increased the cell viability against harmful conditions and controlled the cellular metabolism.[8] Very recently, we also have demonstrated the formation of degradable shells on

microbial yeast cells with a metal-organic complex of tannic acid (TA) and Fe[III], mimicking the germination process in Nature.[9] In addition to the protective capabilities of the TA-Fe[III] nanocoat against UV-C irradiation, lyticase, and silver nanoparticles, the cell division of the yeast cells was controlled by the stimuli-responsive degradation of the nanocoat.[9]

Although cytoprotective and degradable nanocoats, mimicking the sporulation and germination processes, have been applied to individual yeast cells, the chemical nanocoating of individual mammalian cells has remained a challenge.[8e,f] Because mammalian cells, encased with lipid bilayer membranes, are fragile, it is extremely difficult to treat them with chemical methods; therefore, the coating strategies require more carefully selected materials and processes in chemical sporulation and germination.[10] In this study, individual mammalian cells (HeLa, NIH 3T3 fibroblast, and Jurkat cells) were successfully coated with a cytoprotective and degradable TA-Fe[III] complex by using the cytocompatible conditions that ensured the cell viability (Fig. 1a). Not only did the TA-Fe[III] nanocoat protect the cells against UV irradiation and toxic compounds, but also its stimuli-responsive degradation led to programmed cell proliferation.

NIH 3T3 fibroblast cells were selected as a representative adherent cell, because of their wide use in the studies on cell biology. HeLa cells were chosen as a model of cancerous cells, and Jurkat cells, suspension cells, as a model of therapeutic T cells for potential applications of cell coating to T cell therapy. These three types of cells were also suitable for investigation of cell growth and proliferation, because of their short doubling time. TA, a type of polyphenols found in tea, wine, and chocolate, was used as a coating material in this work because of its chemical versatility, including UV absorption, radical scavenging, and metal-ion complexation.[11] Although the TA-Fe[III] nanocoats have been formed on microbial yeast cells[9] and non-living substrates,[11] such as planar and particulate ones, the vulnerability of mammalian cells strictly require the optimization of coating conditions. In this work, we screened the coating solvents and varied the concentrations of the Fe[III] ions to maximize the viability of the coated

a. Center for Cell-Encapsulation Research, Department of Chemistry, KAIST, Daejeon 34141, Korea. E-mail: ischoi@kaist.ac.kr.
b. Department of Chemistry Education, Korea National University of Education, Chungbuk 28173, Korea. E-mail: sunghoyang@knue.ac.kr.
† Electronic Supplementary Information (ESI) available: Experimental details, LSCM images, and SEM, and TEM images. See DOI: 10.1039/x0xx00000x

mammalian cells. In addition, the number of the coating steps was also varied to investigate the thickness dependency of cytoprotectability.
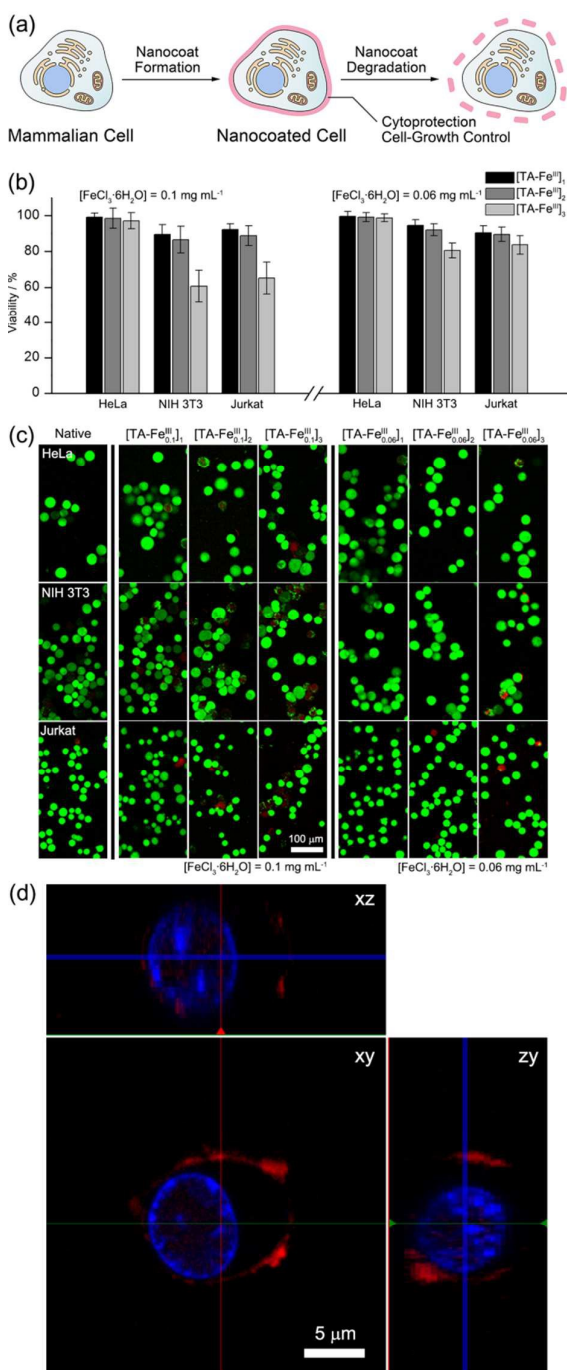

Fig. 1 (a) Schematic representation for controlled formation and degradation of TA-Fe^{III} nanocoats on individual mammalian cells, mimicking sporulation and germination processes. (b) Viability of HeLa, NIH 3T3, and Jurkat cells after coating with TA-Fe^{III}, based on the MTT assay. For the viability test, we used an average of 3 biological replicates, and each sample was tested in triplicate. (c) Live/Dead® cell viability assay of HeLa, NIH 3T3, and Jurkat cells before and after coating. Green: live; red: dead. (d) Z-stacked LSCM images of HeLa@[TA-Fe$_{0.1}^{III}$]$_3$ after treatment with BSA-Alexa Fluor 647 (red). The nuclei were stained with DAPI (blue).

The TA-Fe^{III} nanocoat was formed on individual mammalian cells by simply adding TA and FeCl$_3$ to the cell suspension and incubating the mixture for 10 s. Because of the high affinity of TA to any substrates,[9,11] TA could bind to the cell surface readily. 1,2,3-Trihydroxybenzoyl groups (galloyl groups) of TA formed a metal-organic complex with Fe^{III} ions subsequently, leading to the formation of TA-Fe^{III} nanofilms on the cell surface.[11e] It should be noted that the whole process was performed in serum-free Dulbecco's modified Eagle's medium (DMEM, pH 7.4) for HeLa and NIH 3T3 cells,[10b,c] and in serum-free Rosewell Park Memorial Institute 1640 (RPMI, pH 7.4) for Jurkat cells, after optimization of reaction conditions.

After optimization of the coating medium, we investigated the cell viability with the varied concentrations of FeCl$_3$·6H$_2$O (0.06, 0.1, and 0.2 mg mL^{-1}) and the different numbers of coating steps (1, 2, and 3); the thickness of the TA-Fe^{III} nanofilm was reported to be controlled by the concentration of Fe^{III} ions (but not that of TA)[11e] and the number of coating steps.[9,11b] In this paper, cell@[TA-Fe$_x^{III}$]$_n$ refers to the mammalian cells that were coated n times with TA-Fe^{III}, producing n layers of the nanocoat, with x concentration of the Fe^{III} ions. The viability of each cell type was evaluated with two independent assays: 3-(4,5-dimethylthiazol-2-yl)-2,5-diphenyltetrazolium bromide (MTT) and Live/Dead® staining. MTT, which is reduced to fluorescent formazan in a metabolically active cell, was used to quantify cell viability by measuring the absorbance of the formazan derivative at a specific wavelength (560 nm). The Live/Dead® cell viability assay kit (Life Technologies) contains two fluorescent dyes that differentially stain live and dead cells. Calcein AM, the esterase substrate, stains live cells green, whereas ethidium homodimer-1, the DNA dye, stains dead cells red. Both MTT and Live/Dead® staining assays showed that the cell viability was dependent upon the concentration of the Fe^{III} ions. With 0.2 mg mL^{-1} of the Fe^{III} ions, the viability was 76.1% (n = 1), 57.1% (n = 2), and 30.1% (n = 3) for HeLa cells; 85.1% (n = 1), 53.2% (n = 2), and 37.1% (n = 3) for NIH 3T3 cells; 48.2% (n = 1), , 9.2% (n = 2), and 6.1% (n = 3) for Jurkat cells, based on the MTT assay (Fig. S1). However, the viability increased profoundly with decreased concentrations of the Fe^{III} ions, indicating the potential cytotoxicity of the Fe^{III} ions to mammalian cells; the viability of HeLa@[TA-Fe$_{0.1}^{III}$]$_n$ (n = 1, 2, and 3) was >97% for all the cases based on the MTT assay, and the Live/Dead® staining assay also showed that HeLa@[TA-Fe$_{0.1}^{III}$]$_n$ maintained high viability as indicated by the predominant emission of green fluorescence (Fig. 1b,c). According to the MTT assay, the viability of the NIH 3T3 and Jurkat cells was 89.4% for NIH@[TA-Fe$_{0.1}^{III}$]$_1$, 86.6% for NIH@[TA-Fe$_{0.1}^{III}$]$_2$, 60.7% for NIH@[TA-Fe$_{0.1}^{III}$]$_3$; 92.2% for Jurkat@[TA-Fe$_{0.1}^{III}$]$_1$, 88.9% for Jurkat@[TA-Fe$_{0.1}^{III}$]$_2$, and 65.3% for Jurkat@[TA-Fe$_{0.1}^{III}$]$_3$ (Fig. 1b). The cell viability was further increased by using 0.06 mg mL^{-1} of the Fe^{III} ions; it was at least >80% for all the combinations. Therefore, the TA-Fe^{III} system was more cytocompatible with mammalian cells than our previously reported silica coating for mammalian cells, where the viability was 76.8% for HeLa cells, 80.6% for NIH 3T3 cells, and 50.8% for Jurkat cells, after single coating.[10c] For further
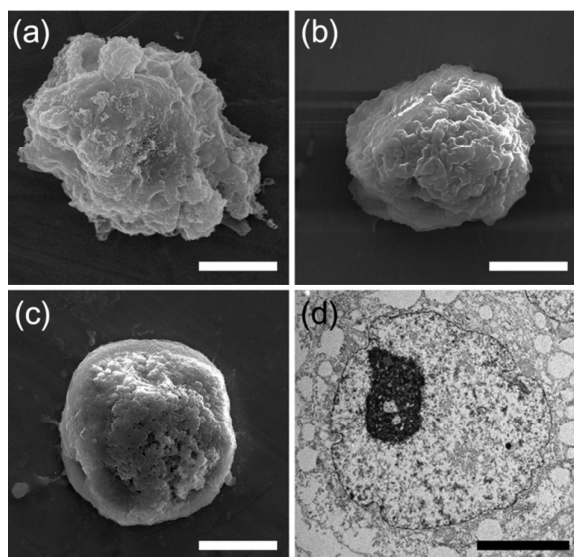
Nanoscale

COMMUNICATION

Fig. 2 SEM micrographs of (a) HeLa@[TA-Fe$_{0.1}^{III}$]$_3$, (b) NIH@[TA-Fe$_{0.1}^{III}$]$_3$, and (c) Jurkat@[TA-Fe$_{0.1}^{III}$]$_3$. (d) TEM micrograph of HeLa@[TA-Fe$_{0.1}^{III}$]$_3$. Scale bar is 5 μm.

Fig. 3 Viability curves of (a) native HeLa, HeLa@[TA-Fe$_{0.1}^{III}$]$_n$, and (b) HeLa@[TA-Fe$_{0.06}^{III}$]$_n$ cells after UV-C irradiation. Graphs of survival ratios versus concentrations of PEI for (c) native HeLa, HeLa@[TA-Fe$_{0.1}^{III}$]$_n$, and (d) HeLa@[TA-Fe$_{0.06}^{III}$]$_n$ cells (n = 1, 2, and 3). The cells were incubated in DMEM at 37.0 °C for 24 h. For the viability test, we used an average of 3 biological replicates, and each sample was tested in triplicate.

studies in this work, we used 0.06 and 0.1 mg mL^{-1} of FeCl$_3$·H$_2$O for nanocoating of mammalian cells.

The formation of the TA-Fe^{III} nanocoat was noticeable with naked eyes, with the coated HeLa cells appearing as purple pellets compared with the native HeLa cells (Fig. S2). The coated cells were characterized by laser-scanning confocal microscopy (LSCM). Because tannic acid was reported to have high binding affinity for proteins,[9] a fluorophore-conjugated protein (bovine serum albumin (BSA)-Alexa Fluor 647) was coupled to the TA-Fe^{III} nanocoat, and the nuclei of the cells were stained with 4',6-diamidino-2-phenylindole (DAPI) for the visualization. The LSCM images clearly showed the cell-in-shell structures for all three types of cells (Fig. S3). In a three-dimensional LSCM analysis, the stained HeLa@[TA-Fe$_{0.1}^{III}$]$_3$ cells were visualized as Z-stacking with a depth of 18.3 μm, separated by 0.3 μm (61 slices). The nuclei of the HeLa cells (blue) were surrounded by BSA-functionalized TA-Fe^{III} film (red), indicating that the TA-Fe^{III} nanocoat was successfully formed over the cell surface (Fig. 1d). The nanocoated mammalian cells were also characterized by scanning electron microscopy (SEM) and energy-dispersive X-ray (EDX) spectroscopy. From the SEM images of the HeLa@[TA-Fe$_{0.1}^{III}$]$_3$, NIH@[TA-Fe$_{0.1}^{III}$]$_3$, and Jurkat@[TA-Fe$_{0.1}^{III}$]$_3$ cells, it was clear that the nanocoated cells maintained their original shape, whereas the native cells were seriously ruptured by dehydration and reduced pressure during sample preparation, indicative of the mechanical durability of the TA-Fe^{III} film (Fig. 2, Fig. S4, and Fig S5). The EDX spectrum of HeLa@[TA-Fe$_{0.1}^{III}$]$_3$, showing the Fe peak at 6.4 keV, also confirmed the successful TA-Fe^{III} formation (Fig. S6). The transmission electron microscopy (TEM) images of microtomed HeLa@[TA-Fe$_{0.1}^{III}$]$_3$ cells showed that the thickness of the [TA-Fe$_{0.1}^{III}$]$_3$ nanocoat was about 35 nm (Fig. 2d; for the TEM image of a microtomed native HeLa cell, see Fig. S7), which was in a good agreement with our previous report.[9]
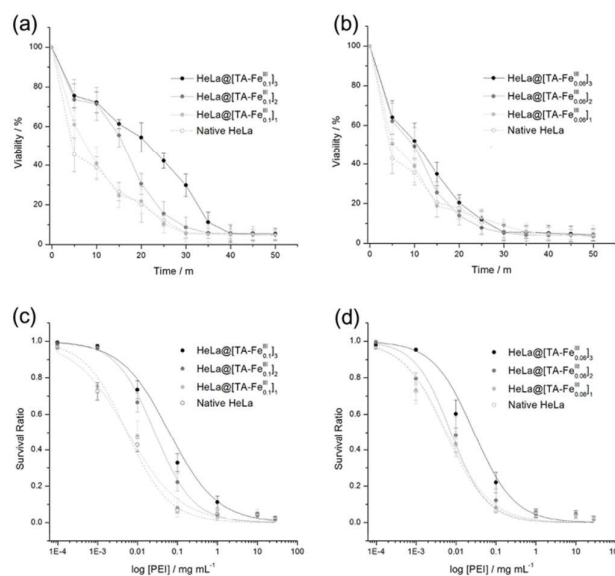
The TA-Fe^{III} nanocoat not only provided structural stability, but also made the coated cells resistant to harmful stresses, such as radiation and chemical stress. UV-C is the electromagnetic radiation that induces lethal stress in living organisms.[12] For example, photosensitive DNA is mutated by exposure to UV-C, resulting in cell death.[13] To evaluate the protective effect of the TA-Fe^{III} nanocoat against UV-C irradiation, HeLa and HeLa@[TA-Fe$_x^{III}$]$_n$ (x = 0.06 and 0.1; n = 1, 2, and 3) were irradiated at 254 nm (power: 4 W), and their viability was measured over time. More than half of the native HeLa cells were dead after 5 min, whereas three quarters of HeLa@[TA-Fe$_{0.1}^{III}$]$_3$ and HeLa@[TA-Fe$_{0.1}^{III}$]$_2$, and 61.0% of HeLa@[TA-Fe$_{0.1}^{III}$]$_1$ survived 5-min UV-C irradiation (Fig. 3a). In other words, as the thickness of the TA-Fe^{III} nanocoat increased, the protective effect against UV-C irradiation also increased. The viability of HeLa@[TA-Fe$_{0.06}^{III}$]$_n$ was measured to be 64.1% for HeLa@[TA-Fe$_{0.06}^{III}$]$_3$, 62.1% for HeLa@[TA-Fe$_{0.06}^{III}$]$_2$, and 50.8% for HeLa@[TA-Fe$_{0.06}^{III}$]$_1$ after 5 min of UV-C irradiation. This less protective capability of HeLa@[TA-Fe$_{0.06}^{III}$]$_n$ also confirmed that the TA-Fe^{III} film played a crucial role in the protection of the HeLa cells against UV-C irradiation. The cytoprotective capability of the TA-Fe^{III} film against UV-C irradiation was also confirmed for NIH 3T3 and Jurkat cells (Fig. S8). The viability of NIH@[TA-Fe$_{0.1}^{III}$]$_3$ was 84.5% after 15-min exposure to UV-C, while that of the native NIH 3T3 cells was 47.3%. The viability of Jurkat@[TA-Fe$_{0.1}^{III}$]$_3$ was 61.8% after 5-min exposure to UV-C, whereas that of the native Jurkat cells was only 21.8%. We believe that the increased protection against UV-C irradiation was attributed to the physicochemical properties of the TA-Fe^{III} film, which filter radiation in the UV-C region.[11e]
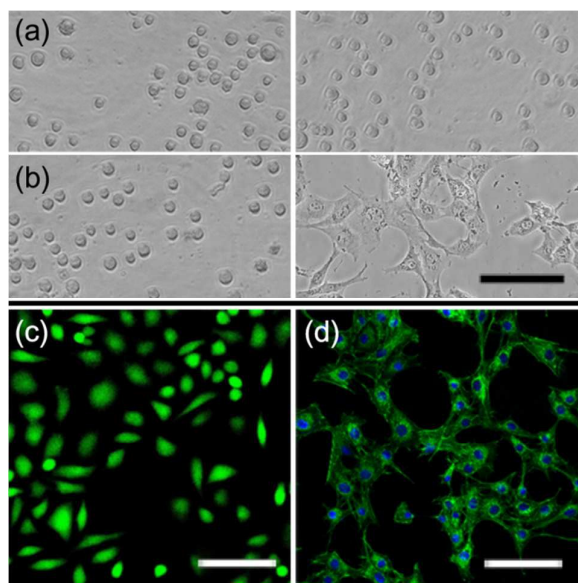
Nanoscale Accepted Manuscript

COMMUNICATION   Nanoscale

Fig. 4 (a) Optical micrographs of HeLa@[TA-Fe$_{0.1}^{III}$]$_3$ (left) immediately after cell seeding and (right) after 96-h culture in DMEM without EDTA. (b-d) Characterizations of HeLa@[TA-Fe$_{0.1}^{III}$]$_3$ in DMEM containing 0.5 mM EDTA: (b) Optical micrographs (left) immediately after cell seeding and (right) after 96-h culture; (c) Live/Dead® cell viability assay after 96-h culture; (d) LSCM micrograph after 96-h culture. F-actin was stained with phalloidin (green) and the nuclei with DAPI (blue). Scale bar is 100 μm.

Cationic polymers are one of the chemical stressors. Because the cell surface is negatively charged, cationic polymers readily attach to the surface *via* electrostatic interactions, causing membrane damage.[14] For example, polyethylenimine (PEI) binds to cell surfaces and penetrates the cells by endocytosis, and long exposure to high concentrations of PEI causes cell death.[15] In this work, native and nanocoated cells were incubated for 24 h in DMEM (for HeLa and NIH 3T3 cells) or RPMI (for Jurkat cells) containing various concentrations of PEI to investigate the cytoprotective capability of the TA-Fe^{III} nanocoat. The concentration of PEI (IC$_{50}$ in mg L^{-1}), at which the survival rate was 0.5,[10c] was 5.46 for native HeLa cells, 62.4 for HeLa@[TA-Fe$_{0.1}^{III}$]$_3$, and 28.2 for HeLa@[TA-Fe$_{0.06}^{III}$]$_3$ (Fig. 3c,d). The IC$_{50}$ value also increased from 24.4 to 135 for NIH@[TA-Fe$_{0.1}^{III}$]$_3$, and from 3.04 to 7.81 for Jurkat@[TA-Fe$_{0.1}^{III}$]$_3$ (Fig. S9).

Another important aspect of the TA-Fe^{III} film was its controlled degradability, which was investigated with the cell culture test. Native HeLa and HeLa@[TA-Fe$_{0.1}^{III}$]$_3$ cells were incubated, respectively, in cell culture flasks under identical culture conditions (37.0 °C with 5% CO$_2$) at equal densities (2.0 × 10^4 cells mL^{-1}). With incubation, the originally round-shaped native HeLa cells adhered to and grew on the flask surface, developing filopodial structures, whereas the HeLa@[TA-Fe$_{0.1}^{III}$]$_3$ cells maintained their spherical shape without any observable attachment to the flask surface (Fig. 4, Fig. S10). The number of the HeLa@[TA-Fe$_{0.1}^{III}$]$_3$ cells remained unchanged after 96 h in culture. Although the viability of HeLa@[TA-Fe$_{0.1}^{III}$]$_3$ decreased from 97.2% to 57.3% after 96 h, the maintenance of both their shape and number indicated that the growth and proliferation of HeLa cells ceased or were

at least suppressed by the TA-Fe^{III} nanocoat. The same retardation of cell growth was observed for the NIH@[TA-Fe$_{0.1}^{III}$]$_3$ and NIH@[TA-Fe$_{0.1}^{III}$]$_3$ cells (Fig. S10). However, the cell growth was resumed in a controlled fashion by degrading the TA-Fe^{III} nanocoat with ethylenediamine tetraacetic acid (EDTA).[11e] After 96 h of incubation in DMEM containing 0.5 mM EDTA, the HeLa@[TA-Fe$_{0.1}^{III}$]$_3$ cells adhered to the culture flask and grew on the surface due to the nanocoat degradation (Fig. 4a,b). After degradation of the TA-Fe^{III} coat, the doubling time of the HeLa cell was measured to be ~19 h (native HeLa: 20 h), which indicated that the proliferation capability of the cells was kept maintained. The Live/Dead® assay and immunocytochemistry analysis showed that the cells were highly viable after adherence and growth (Fig. 4c,d). It should be noted again that the HeLa@[TA-Fe^{III}]$_3$ cells maintained their spherical shape without any adherence after 96 h of culture in the absence of EDTA. These results clearly confirmed that a degradable nanocoat was successfully formed on the cell surface and degraded on demand, mimicking the germination characteristics of the natural spore. The difference could be mentioned that while natural germination is a passive process, the chemical germination is an active process where the coat-degradation timing is controlled chemically.[8e,f]

Conclusions

In summary, we reported a cytocompatible method for forming a degradable nanocoat on individual mammalian cells (HeLa, NIH 3T3, and Jurkat cells) by chemically mimicking the sporulation and germination processes in Nature. The TA-Fe^{III}-coated mammalian cells were reasonably viable and showed greatly enhanced resistance to otherwise lethal agents, such as UV-C and PEI. More importantly, the cell growth and proliferation, suppressed temporarily by the nanocoat, were restored by controlled degradation of the nanocoat. We believe that the remarkable protective capacity and degradability of the TA-Fe^{III} nanocoat would have various single cell-based applications including cell-based sensors, cell therapies, and regenerative medicine, where the temporal cytoprotection of labile mammalian cells is highly required, as well as providing a research platform for fundamental studies in single-cell biology. The concept demonstrated herein also suggests a chemical tool for manipulating the biological activities of mammalian cells, while protecting them with a physically tough nanocoat in *in vitro* situations.

Acknowledgements

Nanoscale Accepted Manuscript

Notes and references

1   (a) D. J. Futuyma, *Evolution 3rd ed.*, Sinauer Associates Inc., Sunderland, MA, USA 2013; (b) K. Donohue, R. R. de Casas, L. Burghardt, K. Kovach and C. G. Willis, *Annu. Rev. Ecol. Evol. Syst.,* 2010, **41**, 293; (c) D. Keilin, *Proc. Roy. Soc. Lond. B,* 1959, **150**, 149.

2   (a) C. M. Kelly, *Microbiology: A Systems Approach 3rd ed.*, McGraw-Hill, New York, USA 2012; (b) P. T. McKenney, A. Driks and P. Eichenberger, *Nat. Rev. Microbiol.,* 2012, **11**, 33; (c) A. O. Henriques and C. P. Moran, Jr., *Annu. Rev. Microbiol.,* 2007, **61**, 555; (d) S. Ghosh, B. Setlow, P. G. Wahome, A. E. Cowan, M. Plomp, A. J. Malkin and P. Setlow, *J. Bacteriol.,* 2008, **190**, 6741; (e) A. Driks, *Trends Microbiol.,* 2002, **10**, 251.

3   (a) D. Hong, H. Lee, E. H. Ko, J. Lee, H. Cho, M. Park, S. H. Yang and I. S. Choi, *Chem. Sci.,* 2015, **6**, 203; (b) J. H. Park, I. S. Choi and S. H. Yang, *Chem. Commun.,* 2015, **51**, 5523; (c) W. Xiong, Z. Yang, H. Zhai, G. Wang, X. Xu, W. Ma and R. Tang, *Chem. Commun.,* 2013, **49**, 7525; (d) S. H. Yang, K.-B. Lee, B. Kong, J.-H. Kim, H.-S. Kim and I. S. Choi, *Angew. Chem. Int. Ed.,* 2009, **48**, 9160.

4   (a) E. H. Ko, Y. Yoon, J. H. Park, S. H. Yang, D. Hong, K.-B. Lee, H. K. Shon, T. G. Lee and I. S. Choi, *Angew. Chem. Int. Ed.,* 2013, **52**, 12279; (b) S. H. Yang, E. H. Ko and I. S. Choi, *Langmuir,* 2012, **28**, 2151; (c) V. G. Kessler, G. A. Seisenbaeva, M. Unell and S. Håkansson, *Angew. Chem. Int. Ed.,* 2008, **47**, 8506.

5   S. A. Konnova, I. R. Sharipova, T. A. Demina, Y. N. Osin, D. R. Yarullina, O. N. Ilinskaya, Y. M. Lvov and R. F. Fakhrullin, *Chem. Commun.,* 2013, **49**, 4208.

6   (a) B. Wang, G. Wang, B. Zhao, J. Chen, X, Zhang and R. Tang, *Chem. Sci.,* 2014, **5**, 3463; (b) S. H. Yang, S. M. Kang, K.-B. Lee, T. D. Chung, H. Lee and I. S. Choi, *J. Am. Chem. Soc.,* 2011, **133**, 2795.

7   (a) S. H. Yang, J. Choi, L. Palanikumar, E. S. Choi, J. Lee, J. Kim, I. S. Choi and J.-H. Ryu, *Chem. Sci.,* 2015, **6**, 4698; (b) J. Lee, S. H. Yang, S.-P. Hong, D. Hong, H. Lee, H.-Y. Lee, Y.-G. Kim and I. S. Choi, *Macromol. Rapid Commun.,* 2013, **34**, 1351; (c) I. Drachuk, O. Shchepelina, M. Lisunova, S. Harbaugh, N. Kelley-Loughnane, M. Stone and V. V. Tsukruk, *ACS Nano,* 2012, **6**, 4266.

8   (a) D. Hong, E. H. Ko and I. S. Choi, in *Cell Surface Engineering: Fabrication of Functional Nanoshells,* ed. R. F. Fakhrullin, I. S. Choi and Y. M. Lvov, Royal Society of Chemistry, Cambridge, UK 2014, Ch. 8; (b) J. H. Park, S. H. Yang, J. Lee, E. H. Ko, D. Hong and I. S. Choi, *Adv. Mater.,* 2014, **26**, 2001; (c) W. Chen, G. Wang and R. Tang, *Nano Res.,* 2014, **7**, 1404; (d) I. Drachuk, M. K. Gupta and V. V. Tsukruk, *Adv. Funct. Mater.,* 2013, **23**, 4437; (e) D. Hong, M. Park, S. H. Yang, J. Lee, Y.-G. Kim and I. S. Choi, *Trends Biotechnol.,* 2013, **31**, 442; (f) S. H. Yang, D. Hong, J. Lee, E. H. Ko and I. S. Choi, *Small,* 2013, **9**, 178; (g) R. F. Fakhrullin, A. I. Zamaleeva, R. T. Minullina, S. A. Konnova and V. N. Paunov, *Chem. Soc. Rev.,* 2012, **41**, 4189; (h) R. F. Fakhrullin and Y. M. Lvov, *ACS Nano,* 2012, **6**, 4557.

9   J. H. Park, K. Kim, J. Lee, J. Y. Choi, D. Hong, S. H. Yang, F. Caruso, Y. Lee and I. S. Choi, *Angew. Chem. Int. Ed.,* 2014, **53**, 12420.

10 (a) V. Kozlovskayam, B. Xue, W. Lei, L. E. Padgett, H. M. Tse and E. Kharlampieva, *Adv. Healthcare Mater.,* 2015, **4**, 686; (b) J. Lee, I. S. Choi and S. H. Yang, *Bull. Korean Chem. Soc.,* 2015, **36**, 1278; (c) J. Lee, J. Choi, J. H. Park, M.-H. Kim, D. Hong, H. Cho, S. H. Yang and I. S. Choi, *Angew. Chem. Int. Ed.,* 2014, **53**, 8056; (d) A. Matsuzawa, M. Matsusaki and M. Akashi, *Langmuir,* 2013, **29**, 7362; (e) A. Nishiguchi, H. Yoshida, M. Matsusaki and M. Akashi, *Adv. Mater.,* 2011, **23**, 3506; (f) N. G. Veerabadran, P. L. Goli, S. S. Stewart-Clark, Y. M. Lvov and D. K. Mills, *Macromol. Biosci.,* 2007, **7**, 877.

11 (a) S. Kim, S. Kwak, S. Lee, W. K. Cho, J. K. Lee and S. M. Kang, *Chem. Commun.,* 2014, **51**, 5340; (b) S. Kim, D. S. Kim and S. M. Kang, *Chem. Asian J.,* 2014, **9**, 63; (c) J. Guo, Y. Ping, H. Ejima, K. Alt, M. Meissner, J. J. Richardson, Y. Yan, K. Peter, D. v. Elverfeldt, C. E. Hagemeyer and F. Caruso, *Angew. Chem. Int. Ed.,* 2014, **53**, 5546; (d) M. A. Rahim, H. Ejima, K. L. Cho, K. Kempe, M. Müllner, J. P. Best and F. Caruso, *Chem. Mater.,* 2014, **26**, 1645; (e) H. Ejima, J. J. Richardson, K. Liang, J. P. Best, M. P. v. Koeverden, G. K. Such, J. Cui and F. Caruso, *Science,* 2013, **341**, 154.

12 (a) T. A. Slieman and W. L. Nicholson, *Appl. Environ. Microbiol.,* 2001, **67**, 1274; (b) R. M. Tyrrell, *Mol. Aspects Med.,* 1994, **15**, 1.

13 (a) F. E. Quaite, B. M. Sutherland and J. C. Sutherland, *Nature,* 1992, **358**, 577; (b) R. P. Sinha and D.-P. Häder, *Photochem. Photobiol. Sci.,* 2002, **1**, 225.

14 Y. Teramura and H. Iwata, *Soft Matter,* 2010, **6**, 1081.

15 (a) D. W. Pack, A. S. Hoffman, S. Pun and P. S. Stayton, *Nat. Rev. Drug Discovery,* 2005, **4**, 581; (b) D. Putnam, C. A. Gentry, D. W. Pack and R. Langer, *Proc. Natl. Acad. Sci. USA,* 2001, **98**, 1200.

Nanoscale Accepted Manuscript